ACS APPLIED MATERIALS & INTERFACES

www.acsami.org

Research Article

Synthesis Control of Charge Separation at Anatase TiO_2 Thin Films Studied by Transient Surface Photovoltage Spectroscopy

Thomas Dittrich,* Jekaterina Sydorenko, Nicolae Spalatu,* Norbert H. Nickel, Arvo Mere, Malle Krunks, and Ilona Oja Acik

Cite This: *ACS Appl. Mater. Interfaces* 2022, 14, 43163–43170

Read Online

ACCESS | Metrics & More | Article Recommendations | Supporting Information

ABSTRACT: For the efficient photocatalytic oxidation of organic pollutants at surfaces of semiconductors, photogenerated holes shall be separated toward the surface and transferred to reactive surface sites, whereas the transfer of photogenerated electrons toward the surface shall be minimized. In this Research Article, the identification of suitable synthesis control of charge separation combined with an in-depth understanding of charge kinetics and trapping passivation mechanisms at the related surfaces can provide tremendous opportunities for boosting the photocatalytic performance. In this work, a comprehensive transient surface photovoltage spectroscopy study of charge separation at anatase TiO_2 thin films, synthesized by ultrasonic spray pyrolysis from titanium(IV) isopropoxide (TTIP)−acetylacetone (AcacH) based precursor is reported. By varying the amount of AcacH in the precursor solution, an experimental approach of synthesis control of the charge transfer toward TiO_2 surface is provided for the first time. An increased amount of AcacH in the precursor promotes transition from preferential fast electron to preferential fast hole transfer toward anatase surface, correlating with a strong increase of the photocatalytic decomposition rate of organic pollutants. Suitable mechanisms of AcacH-induced passivation of electron traps at TiO_2 surfaces are analyzed, providing a new degree of freedom for tailoring the properties of photocatalytic systems.

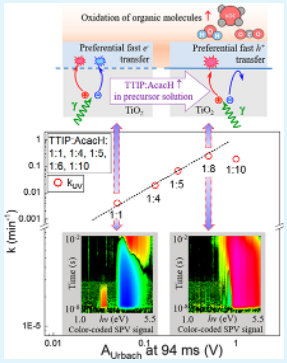

KEYWORDS: *TiO_2, charge separation, photocatalytic activity, surface photovoltage, transient spectroscopy*

1. INTRODUCTION

For the initiation of photocatalytic reactions at surfaces of semiconductors, for example at TiO_2, photogenerated electrons and holes shall be separated toward the external surface and transferred to reactive surface sites. Photogenerated electrons and holes transferred toward reactive surface sites are responsible for photocatalytic reduction (or inhibition of oxidation) or oxidation (or inhibition of reduction), respectively. The investigation of limiting processes is important for a deeper understanding of photocatalytic reactions at semiconductor surfaces and for the further development and optimization of photocatalytic systems.

The discovery by Fujishima and Honda in 1972 of water splitting with a photoirradiated titania electrode opened a new field in photocatalysis and highly stimulated the research interest in this field.[1] Some of the most important applications of photocatalysis are in the area of environmental remediation. Hydroxyl radicals produced during illumination of photocatalytic materials can be used for decomposition of organic molecules adsorbed on so-called self-cleaning surfaces. Organic pollutants dispersed in water, air, or soil can also be destroyed by photocatalytic oxidation.

TiO_2 is a wide band gap photocatalyst, and thus, it needs ultraviolet (UV) light for excitation of photogenerated charge carriers and high photocatalytic activity.[2] There are innumerable permutations of research aimed to increase the absorption of visible (VIS) light and the corresponding photocatalytic performance of TiO_2, for example, by doping/codoping, dye sensitization, or implementation of heterojunctions. However, the VIS light sensitization of photocatalysts remains a major challenge in the field.[3,4] Therefore, further steps in material synthesis, understanding and process optimization are needed to broaden applications of photocatalytic systems, also from an economic point of view.

Different properties of materials can play a significant role in determining their photocatalytic activity. For example, surface states and facet orientations play an important role for adsorption of reactants and charge transfer during photoreactions.[5,6] In turn, diffusion and recombination of photogenerated charge carriers depend on the average size of nanoparticles or grains and grain boundaries.[7] Photoinduced surface defects, such as oxygen vacancies, can act as trapping sites for charge carriers, which reduce the mobility, and reactivity of photogenerated holes.[8] Moreover, pretreatment of TiO_2 surfaces with UV light enhances the production of active

Received: May 30, 2022
Accepted: September 2, 2022
Published: September 13, 2022

sites even for photocatalytic purification processes driven by VIS light. The surface of TiO_2 is modified during absorption of UV light and a metastable surface structure is formed, which is closely related to the reverse superhydrophilic properties.[9]

The influence of organic additives for the formation of anatase TiO_2 has been studied for many years, especially in relation to the preparation of nanoporous anatase matrixes for dye-sensitized solar cells[10] and to photocatalysis.[11] Stabilization of titanium(IV) isopropoxide (TTIP) with acetylacetone (AcacH) and effects of AcacH on the film properties have been studied by several authors.[12−14] Recently, it has been shown that the increase of the AcacH molar ratio in precursor solutions can increase the photocatalytic activity of the TiO_2 films.[15] For example, a change of the TTIP: AcacH molar ratio from 1:4 to 1:8 resulted in an increase of the photodegradation reaction-rate constant under UV light by about a factor of 10.[15] At the same time, an increase of the concentration of carbon species was observed at the TiO_2 surfaces by X-ray photoelectron emission spectroscopy (XPS).[15] Therefore, the enhanced photocatalytic performance was tentatively explained by the effect of carbon species on the surface of TiO_2 films. However, the cause of the influence of AcacH in the precursor solution on the photocatalytic activity of anatase TiO_2 films remains unclear.

Surface photovoltage (SPV) signals arise due to separation of photogenerated charge carriers in space (see, for example, the review[16]). In contrast to other techniques, SPV gives specific information about the direction of charge separation. Usually, positive or negative signs of SPV signals are related to preferential separation of positive or negative charge toward the external surface. Charge separation can be driven by different processes, such as drift in built-in electrical fields or asymmetric trapping (see for details also ref 19). Furthermore, a sign can change during an SPV transient, for example, if electrons and holes are trapped both at the surface whereas the charge carriers with the highest trap density relax faster than the charge carriers with the lowest trap density. Transient SPV spectroscopy[17−19] is based on the measurement of SPV signals as functions of photon energy and relaxation time. This allows to select contributions to SPV signals with opposite sign and, therefore, gives the opportunity to distinguish between the relaxation in certain time domains of electrons or holes which have been preferentially transferred toward the external surface. In this work, the spectral range of transient SPV spectroscopy was extended to 5.5 eV. The measurements were performed with a perforated electrode and a charge amplifier.[20]

By applying transient surface photovoltage spectroscopy, we showed for the first time that trapping of electrons at anatase TiO_2 thin films can be minimized by increasing the amount of acetylacetone (AcacH) in the titanium(IV) isopropoxide (TTIP) precursor solution—a widely used precursor by many research groups for synthesis of TiO_2. The passivation of electron traps at the surface of anatase TiO_2 films correlated with a strong increase of photodegradation rate constants. These results open a new way to unravel limiting electronic processes not only at photocatalytic surfaces but also at other kinds of surfaces and buried interfaces.

2. EXPERIMENTAL SECTION

Anatase TiO_2 thin films were synthesized by ultrasonic spray pyrolysis from mixtures of titanium(IV)isopropoxide (TTIP, Sigma-Aldrich) as a titanium source, acetylacetone (AcacH, Sigma-Aldrich) as a stabilizing agent, and ethanol as a solvent (see for details also ref 15). After deposition on glass substrates at 350 °C, the layers were annealed at 500 °C in air for 1 h. The TTIP: AcacH molar ratio ratio was changed between 1:1 and 1:20. The mean crystallite size of anatase TiO_2 was on the order of 40 nm for all layers and the layers had a thickness of 300 to 400 nm.[15] All films irrespective of the amount of AcacH in the precursor solution showed reversed photoinduced superhydrophilic properties after 15 min of UV-A irradiation (Table S1). Moreover, photoinduction of TiO_2 surface with UV-A treatment before experiments strongly enhanced the photocatalytic activity under VIS light (Figure S1). Secondary-ion-mass spectrometry (SIMS) measurements showed a correlation of the carbon distribution with the spray cycles whereas the absolute concentrations of carbon atoms is independent of the TTIP: AcacH ratio (Figure S2).

Before performing transient SPV spectroscopy measurements, the samples were compared by the measurements of the light induced change of the contact potential difference (ΔCPD) with a Kelvin probe (Besocke delta phi) in air. For illumination, a Xe lamp with a quartz prism monochromator (SPM2, Carl Zeiss Jena) was used.

A preparation of charge-selective contacts is not necessary for obtaining SPV signals on a thin film. In the study at hand, for the TiO_2/glass system, there are two interfaces: (i) the interface between glass and TiO_2 layer and (ii) the interface between TiO_2 and environment (free surface of TiO_2 films). The interface between glass and the TiO_2 layer has much lower trap density than the free surface, making the asymmetry for getting the SPV signal. The free surface is exposed to molecules and the defect density/trap density at the free surface is much higher so that it allows to probe the changes at the external free surface.

SPV transients were excited with laser pulses from a tunable Nd:YAG laser (NT230-50, λ = 216−2600 nm) that is equipped with a spectral cleaning unit, EKSPLA The laser pulses had a width of 3−5 ns, and the photon flux was nearly constant between about 2.4 and 4 eV (see Figure S3 and for more details see ref 18).

SPV transients were measured with a fixed perforated electrode, a charge amplifier (Electronik Manufaktur Mahlsdorf, resolution time 7 ns) and an oscilloscope card (Gage, CSE 1622-4GS). The SPV signal height was calibrated with a periodic square wave signal (1 V_{PP}) applied at the back side of the sample (for more details see ref 20). The repetition rate of the laser pulses was 1 Hz and 10 transients were averaged. SPV signals were analyzed as the difference to signals of a bare substrate to discriminate parasitic background.

3. RESULTS AND DISCUSSION

3.1. DC (Kelvin Probe) SPV Spectroscopy. Figure 1 shows the spectra of ΔCPD for layers of anatase TiO_2

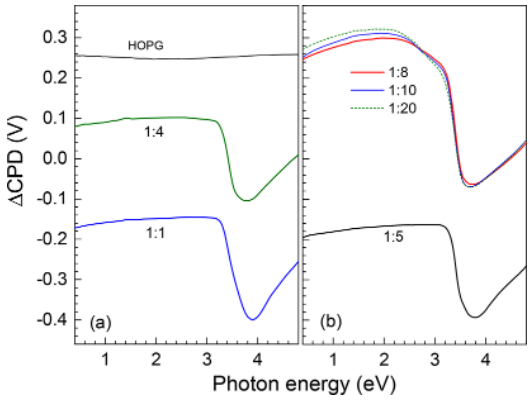

Figure 1. Spectra of the contact potential difference for layers of anatase TiO_2 thin films synthesized with TTIP: AcacH = 1:1 and 1:4 (a, green and blue lines, respectively) and 1:5, 1:8, 1:10, and 1:20 (b, black, red, blue, and dashed green lines, respectively). HOPG is shown for comparison.

https://doi.org/10.1021/acsami.2c09032
ACS Appl. Mater. Interfaces 2022, 14, 43163−43170

synthesized with TTIP: AcacH = 1:1, 1:4, 1:5, 1:8, 1:10, and 1:20. Highly oriented pyrolytic graphite (HOPG) is shown for comparison. The ΔCPD of HOPG did not show an influence of illumination. For HOPG, the value of ΔCPD was about 0.26 V, which corresponds to the work function (WF) of HOPG. At low photon energies, the values of ΔCPD were about −0.17, 0.08, −0.19, 0.247, 0.254, and 0.273 V for TTIP: AcacH of 1:1, 1:4, 1:5, 1:8, 1:10, and 1:20, respectively. In air, the WF of HOPG can be used as a reference (WF of HOPG in air: 4.475 eV).[21] Therefore, the values of WF were 4.045, 4.295, 4.025, 4.462, 4.469, and 4.488 eV for TiO_2 thin films prepared at TTIP: AcacH of 1:1, 1:4, 1:5, 1:8, 1:10, and 1:20, respectively. The changes of the WF of anatase TiO_2 thin films is in qualitative agreement with the shift of the valence band in X-ray photoelectron spectroscopy (XPS) measurements.[22] The values of WF for TiO_2 thin films prepared at TTIP: AcacH of 1:8, 1:10, and 1:20 were larger than for the other films and very similarly. In contrast, the values of WF for TiO_2 thin films prepared at TTIP: AcacH of 1:1, 1:4, and 1:5 scattered significantly. Therefore, the surface dipole formed on TiO_2 thin films prepared at TTIP: AcacH of 1:8, 1:10, and 1:20 was practically constant, whereas the negative surface charge was larger than for the other films.

Strong changes of the slopes of the ΔCPD spectra of anatase (Figure 1) set on at about 3.2 eV, which usually referred to the band gap of anatase TiO_2. The change of the slope of the ΔCPD is related to the evolution of SPV signals, whereas the signs of the light induced ΔCPD and SPV are opposite. The corresponding maximum SPV signals were reached at photon energies between about 3.7 and 3.9 eV and amounted, with respect to ΔCPD at the lowest photon energies, to 0.23, 0.185, 0.202, 0.309, 0.323, 0.342 V for TTIP: AcacH = 1:1, 1:4, 1:5, 1:8, 1:10, and 1:20, respectively. Therefore, photogenerated electrons and holes were preferentially separated toward the bulk and external surface of the layers of anatase, respectively, whereas charge separation was stronger for TTIP: AcacH of 1:8, 1:10, and 1:20 than for 1:1, 1:4, and 1:5. However, this overall charge separation does not give specific information about fast and local processes of charge separation, which are most important for photocatalysis.

3.2. Contour Plots of Transient SPV Spectroscopy. Figure 2 shows the contour plots of transient SPV spectroscopy, that is, the color-coded SPV signals as a map in photon energy and time, for TTIP: AcacH of 1:1, 1:4, 1:5, 1:8, 1:10, and 1:20. For TTIP: AcacH of 1:1, negative SPV signals set at around 3.1 eV and reached values up to more than −100 mV in the spectral range between about 3.4 and 4 eV for times shorter than 10 μs. At longer times (from about 10 ms at 3.3 eV to about 100 μs at 4.8 eV), the sign of the SPV signals changed to positive and positive signals were measured up to the order of 20 mV at longer times and higher photon energies. Below the band gap, positive SPV signals appeared between 2 and 2.5 eV at times up to about 1 μs.

For TTIP: AcacH = 1:4, negative SPV signals appeared as well but in a narrower spectral range between about 3.2 and 3.7 eV and for times up to about 1 ms. At longer times, positive SPV signals were observed in this spectral range and over the whole time domain at higher photon energies. For TTIP: AcacH = 1:5, small negative signals up to about −20 mV appeared in a range between about 3.2 and 3.6 eV for times up to about 20 μs and positive SPV signals were measured at longer times and in the whole domain for photon energies above 3.6 eV, whereas positive SPV signals set on at longer times at photon energies of about 2.8 eV.

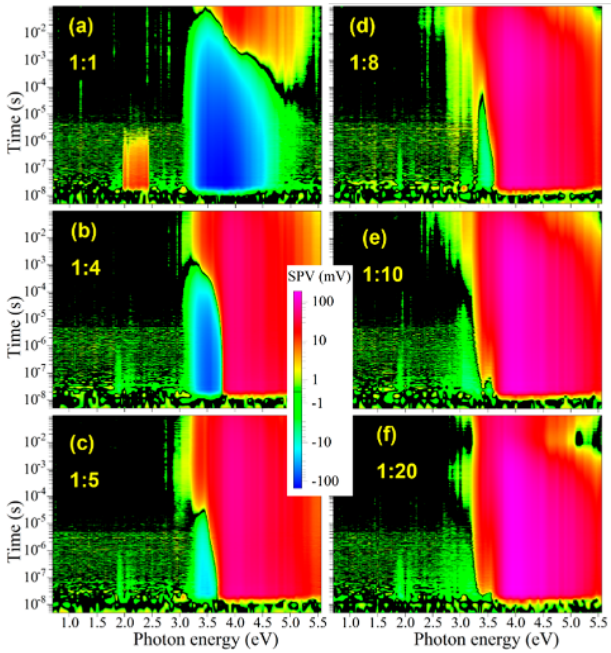

Figure 2. Contour plots of transient SPV spectroscopy for layers of anatase TiO_2 thin films synthesized with TTIP: AcacH = 1:1, 1:4, 1:5, 1:8, 1:10, and 1:20 (a−f, respectively). Remark: A contour plot shows the color-coded SPV signals as a map in photon energy and time. Note the logarithmic color scale for the SPV signals.

For TTIP: AcacH = 1:8, very small negative signals up to about −5 mV still appeared for times up to about 20 μs at 3.4 eV. At longer times, positive SPV signals set on at photon energies of about 2.4 eV and the positive SPV signals reached values up to about 100 mV. Only a tiny rest of negative SPV signals appeared in the contour plot for TTIP: AcacH = 1:10 whereas it was very similar to that for TTIP: AcacH = 1:8 in the other parts. Incidentally, regarding the reproducibility of preparation and measurements, Figure S4 compares the contour plots of transient SPV spectroscopy for the first and second series of the films with TTIP:AcacH 1:8 synthesized in the same way in the different times. A comparison between panels a and b shows the excellent reproducibility of the preparation. After annealing, the amount of electron traps as well as of electronic states in the band gap of anatase increased. For TTIP: AcacH = 1:20, negative SPV signals of up to about 1−2 mV were observed only between 3.3 and 3.6 eV for times shorter than about 30 ns. Furthermore, the highest positive SPV signals of up to about 170 mV were measured for TTIP: AcacH = 1:20. In addition, the positive SPV signals decreased drastically for TTIP: AcacH = 1:20 at photon energies above 5 eV and times longer than 2−3 ms.

3.3. Spectral Analysis and Correlation of Urbach Tails with Decomposition Rates. SPV spectra were extracted from the contour plots at times of 30 ns, 10 μs, 1 ms, and 94 ms after switching on the laser pulses (see Figure 3) and are given for layers of anatase TiO_2 synthesized with TTIP: AcacH = 1:1, 1:4, 1:5, 1:8, and 1:20 (a−e, respectively). At the shortest times for TTIP: AcacH = 1:1 and at the longest times for TTIP: AcacH = 1:20, the negative and positive SPV signals increased exponentially at the onsets and were fitted with a characteristic tail energy of E_t = 60 meV. This tail energy is

https://doi.org/10.1021/acsami.2c09032
ACS Appl. Mater. Interfaces 2022, 14, 43163−43170

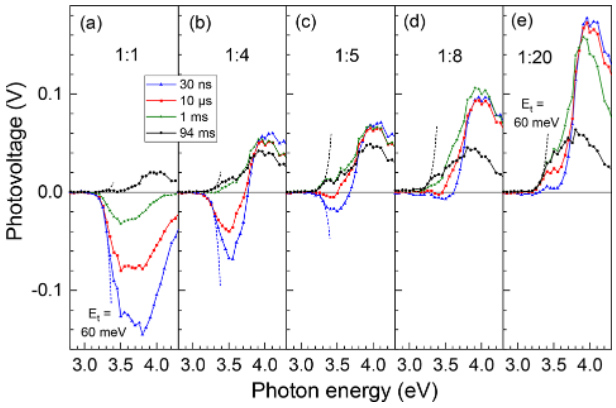

Figure 3. SPV spectra for layers of anatase TiO_2 thin films synthesized with TTIP: AcacH = 1:1, 1:4, 1:5, 1:8, and 1:20 (a−e, respectively) obtained at times of 30 ns, 10 μs, 1 ms, and 94 ms after switching on the laser pulses (black, red, blue, and green lines, respectively). The dotted blue and dashed black lines correspond to exponential tails with E_t = 60 meV at 30 ns and 94 ms, respectively. The value of E_t was obtained by fitting for TTIP:AcacH = 1.1 (at 30 ns) and 1:20 (at 94 ms).

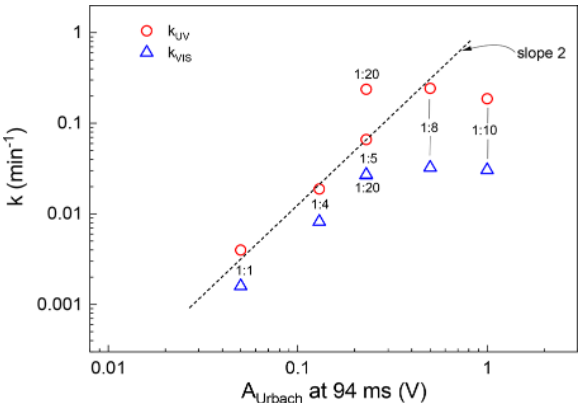

Figure 4. Correlation plots between A_{Urbach} measured at 94 ms and the photocatalytic degradation rates of stearic acid under illumination in UV-A and visible light (k_{UV} and k_{VIS}, red circles and blue triangles, respectively). The values of k_{UV} and k_{VIS} were reproduced from ref 15. Copyright 2019, MDPI open access Creative Commons CC BY 4.0 license. The numbers correspond to the TTIP: AcacH ratios.

close to that of anatase single crystals, depending also on polarization,[23] what gives evidence for one dominating mechanism of charge separation. Furthermore, other onsets of the SPV signals can also be treated by an exponential increase with E_t = 60 meV (see the dashed and dotted lines in Figure 3).

Most of the onset regions of SPV signals are characterized by the low signals case with one dominating mechanism of charge separation, i.e., the SPV signals are proportional to the generation rate or absorption coefficient. Closer to the indirect or optical band gap (E_{ig} = 3.46 eV[24] or E_{og} = 3.42 or 3.46 eV depending on polarization,[23] respectively), the low signal case is no longer valid and dominating mechanisms of charge separation can change. For example, a change from negative toward positive SPV signals set on slightly above E_{ig} at 30 ns and 10 μs for TTIP: AcacH = 1:4, 1:5, 1:8, and 1:20 and at 1 ms for TTIP: AcacH = 1:1, whereas even the sign did change for TTIP: AcacH = 1:4, 1:5, and 1:8. Furthermore, a change from negative toward positive SPV signals set on above 3.8 eV at 30 ns and 10 μs for TTIP: AcacH = 1:1. For the other samples and times, a steep increase toward more positive SPV signals was observed above 3.8 eV what is close to the direct band gap of anatase (3.97 eV).[24]

For photocatalytic oxidation reactions, photogenerated holes shall be separated toward the external surface, i.e., corresponding SPV signals shall be positive. Positive SPV signals were observed for all samples at 94 ms. As a parameter, the amplitude of the exponential onset of positive SPV signals (A_{Urbach}) measured at 94 ms was correlated with the degradation rates of stearic acid under illumination in UV-A and visible light (k_{UV} and k_{VIS}, red circles and blue triangles, respectively) in Figure 4 (values were taken from ref 15). A square dependence of k_{UV} and k_{VIS} on A_{Urbach} was found for TTIP: AcacH = 1:1, 1:4, 1:5, and 1:8 and for TTIP: AcacH = 1:1, 1:4, and 1:5. Therefore, k_{UV} and k_{VIS} were limited by photogeneration in these regions. At higher values of TTIP: AcacH, the degradation rates saturated, i.e., limitation by photogeneration changed to limitation by another process as, for example, charge transfer rates into reactive species adsorbed at the surface of anatase nanoparticles.

3.4. Transient Analysis and Correlation of Back Transfer Rates with Decomposition Rates.

For getting a deeper insight into processes of charge separation and relaxation, SPV transients were selected at characteristic energies of 2.4, 3.3, 3.6, and 4.0 eV. The absorption lengths in anatase are about 10 μm,[23] 300 nm, and 30 nm[25] at the photon energies of 3.3, 3.6, and 4.0 eV, respectively. Therefore, excitation at the photon energies of 3.3, 3.6, and 4.0 eV corresponded to homogeneous absorption across the whole anatase layer, to homogeneous absorption across the first monolayers of anatase TiO_2 crystallites and to preferential absorption within the first monolayer of crystallites in the thin films, respectively.

Figure 5 shows the SPV transients excited at characteristic energies of 2.4, 3.3, 3.6, and 4.0 eV for layers of anatase nanoparticles synthesized with TTIP: AcacH = 1:1, 1:4, 1:5, 1:8, and 1:20 (a−e, respectively). For excitation at 2.4 eV, a transient appeared only for TTIP: AcacH = 1:1. For excitation at 3.3 eV, the amplitudes at about 20 ns after the onsets of the

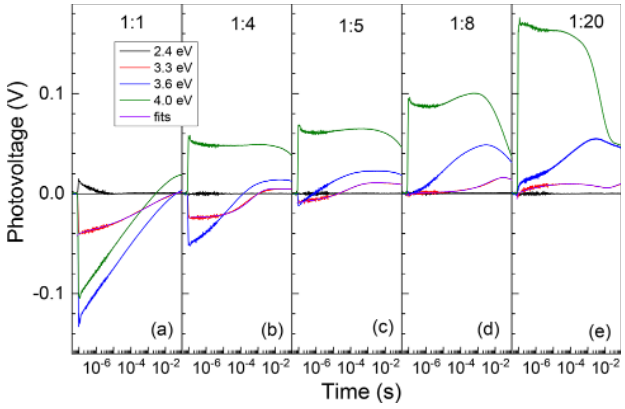

Figure 5. SPV transients for layers of anatase TiO_2 thin films synthesized with TTIP: AcacH = 1:1, 1:4, 1:5, 1:8, and 1:20 (a−e, respectively) excited at photon energies of 2.4, 3.3, 3.6, and 4.0 eV (black, red, blue, and green lines, respectively). The onsets of the laser pulses were shifted to 80 ns in order to show the baseline on the logarithmic time scale. The solid pink lines are fits for excitation at 3.3 eV according to eq 1.

https://doi.org/10.1021/acsami.2c09032
ACS Appl. Mater. Interfaces 2022, 14, 43163−43170

laser pulses decreased from −40 to −24, −8, and about −1 and −2 mV and the time at which the sign of the SPV signals changed to positive from 40 to 1 ms, 20 μs, and about 30 and 30 ns (after switching on the laser pulses) for TTIP: AcacH = 1:1, 1:4, 1:5, 1:8, and 1:20, respectively. For excitation at 3.6 eV, the amplitudes at about 20 ns after the onsets of the laser pulses changed from −130 to −51, −12, and about −1 and 0 mV for TTIP: AcacH = 1:1, 1:4, 1:5, 1:8, and 1:20, respectively, whereas the time at which the sign changed from negative to positive became shorter for TTIP: AcacH = 1:4 and 1:5. For excitation at 4.0 eV, the amplitudes at about 20 ns after the onsets of the laser pulses changed strongly from −104 to +57, +68, +95, and +175 mV for TTIP: AcacH = 1:1, 1:4, 1:5, 1:8, and 1:20, respectively.

With respect to the facts of homogeneous absorption and small signals case for excitation at 3.3 eV, it is reasonable to fit the related SPV transients. SPV transients with only one component can often be fitted by stretched exponentials, for example, when relaxation is dominated by tunneling steps from localized states (see, for example ref 26). Fitting of SPV transients with a minimum number of components gives information about limiting processes involved in charge separation and relaxation. The transients excited at 3.3 eV could be well fitted with one positive and one negative stretched exponentials for TTIP: AcacH = 1:4, 1:5, and 1:8 (amplitudes, time constants, and stretching parameters for negative and positive components are denoted by A_e and A_h, τ_e and τ_h, and β_e and β_h in equation 1, respectively). An additional logarithmic decay factor ($C_1(t)$) was needed for fitting the negative stretched exponential component for TTIP: AcacH = 1:1. A logarithmic decay is close to relaxation limited by distant dependent tunneling recombination.[27] Furthermore, an additional positive component increasing in time by a (stretched) logistic growth ($C_2(t)$) was needed for fitting the SPV transient for TTIP: AcacH = 1:20. In general, SPV signals can grow in time, for example, due to diffusion.[28] Here, the slow increase of SPV of positive signals for TTIP: AcacH = 1:20 can be assigned to diffusion of electrons toward the bulk of the layer of anatase nanoparticles (interparticle transport limited by trapping).

$$\mathrm{SPV}(t) = -C_1(t)\cdot A_e\cdot\exp\left[-\left(\frac{t}{\tau_e}\right)^{\beta_e}\right] + A_h\cdot\exp\left[-\left(\frac{t}{\tau_h}\right)^{\beta_h}\right] + C_2(t) \quad (1)$$

with

$$C_1(t) = 1 - b\cdot\ln^2\left(1 + \frac{t}{\tau_C}\right) \text{ for TTIP: AcacH} = 1{:}\,1 \quad (1')$$

and

$$C_2(t) = A_L\cdot\left(\frac{1}{1 + \exp\left[-\left(\frac{t}{\tau_L}\right)^{\beta_L}\right]} - \frac{1}{2}\right) \text{ for TTIP: AcacH} = 1{:}\,10 \quad (1'')$$

Additionally, a sum of two negative stretched exponentials was needed for obtaining reasonably well fits of the SPV transients for TTIP: AcacH = 1:8 and 1:10. Fitted transients are shown in Figure 5 for TTIP: AcacH = 1:1, 1:4, 1:5, 1:8, and 1:20. The parameters b, τ_C, A_L, τ_L, and β_L amounted to 0.002, 0.5 ns, 21 mV, 0.2 s, and 0.8, respectively.

The trends of the fitting parameters for the positive and negative stretched exponentials are summarized in Figure 6 for

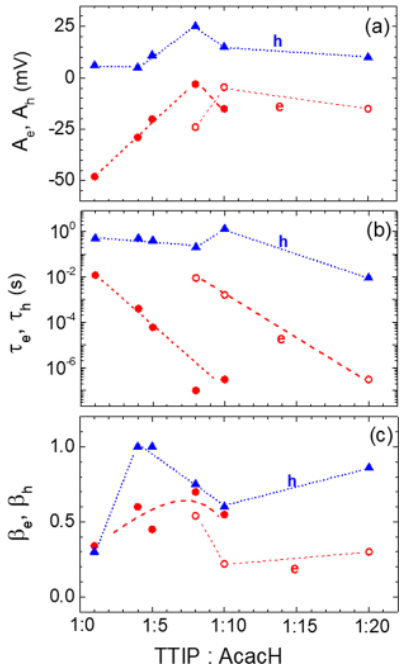

Figure 6. Dependencies of the fit parameters A_e and A_h (a), τ_e and τ_h (b), and β_e and β_h (c) on TTIP:AcacH for the transients measured at 3.3 eV. The red circles and blue triangles in panels a−c are related to the electron and hole components, respectively. The filled and open red circles represent the two components of the negative stretched exponentials regarding to the trends of τ_e. The dotted and dashed lines in panels a−c are guides for the eye.

A_e and A_h (a), τ_e and τ_h (b), and β_e and β_h (c). The most striking difference appeared in the trends of τ_e, which strongly decreased from about 10 ms at TTIP: AcacH = 1:1 to about 0.1−0.3 μs for the fast component at TTIP: AcacH = 1:8 and 1:10 and from about 10 ms for the slow component at TTIP: AcacH = 1:8 to about 0.3 μs at TTIP: AcacH = 1:20. Therefore, the dominating relaxation mechanism of electrons separated in space changed around TTIP: AcacH = 1:8. The values of τ_h were mainly limited by the repetition rate of the laser pulses and ranged, therefore, between about 0.2 to 1 s for TTIP: AcacH = 1:1−1:10, depending also on the stretching parameters and additional slow processes. For TTIP: AcacH = 1:20, τ_h was on the order of 10 ms so that an additional slow process could be observed. It can be supposed that similar additional slow processes were present but masked by the dominating slow relaxation of holes separated toward the external surface for lower values of TTIP: AcacH.

A_e decreased from about −48 mV to −3 mV between TTIP: AcacH = 1:1 and 1:8 which correlates with an increase of the photocatalytic degradation rates of stearic acid in this range.[15] A_h or A_e show a maximum or a local maximum at TTIP: AcacH = 1:8 if considering the sum of the amplitudes of both negative stretched exponentials for TTIP: AcacH = 1:8 and 1:10. In contrast to τ_e, the values of β_e did not show very clear trends. The lowest values of β_e were found for TTIP: AcacH = 1:1, 1:10 (slow component), and 1:20. The highest value of β_e

https://doi.org/10.1021/acsami.2c09032
ACS Appl. Mater. Interfaces 2022, 14, 43163−43170

was obtained for TTIP: AcacH = 1:8 (fast component). Interestingly, β_h showed a strong increase from about 0.3 at TTIP: AcacH = 1:1 to 1 at TTIP: AcacH = 1:4 and 1:5 and a decrease to 0.6 at TTIP: AcacH = 1:10, followed by an increase to 0.86 at TTIP: AcacH = 1:20.

The values of k_{UV} and k_{VIS} are correlated with τ_e in Figure 7. An anticorrelation with a square dependence, i.e., $k_{UV(VIS)} \propto \tau_e^{-2}$ (corresponds to the electron back transfer rate), has been found for TTIP: AcacH = 1:1, 1:4, and 1:5. For TTIP: AcacH = 1:8 and 1:10, the correlation was much weaker. The correlation of the electron back transfer rates with the photocatalytic degradation rates is also similar to the correlation between increasing $k_{UV(VIS)}$ at decreasing A_e (not shown).

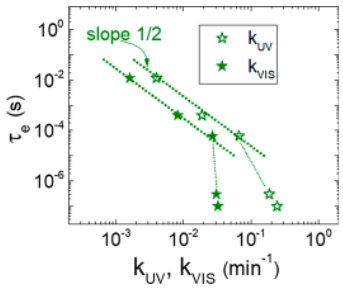

Figure 7. Correlation between k_{UV} and k_{VIS} (open and filled stars, respectively) and τ_e. The values of k_{UV} and k_{VIS} were taken after.[15]

As remark, in principle, fits can also be performed for excitation at higher photon energies. However, components cannot be so obviously assigned to given processes since charge transport shall be considered due to gradients in photogeneration. Furthermore, saturation phenomena can dominate at higher photon energies due to (very) high absorption so that the interpretation of fitting parameters is less straightforward in relation to the photocatalytic activity.

3.5. Suitable Mechanism of AcacH-Induced Passivation of Electron Traps at TiO_2 Surfaces. The experimental results presented above show that the sign of the transient SPV signal changes from negative to positive with increasing TTIP:AcacH ratio. This is directly related to the electron concentration at the surface of the specimens, which is vastly reduced with an increase of the AcacH concentration in the precursor solution. The source of electrons is widely believed to be oxygen vacancies (V_O) that can act as double donors. For rutile and anatase TiO_2, the ionization energies of the (0/+) and (+/2+) adiabatic transitions amount to E_I = 0.1 and 0.4 eV and <0.1 and 0.3 eV, respectively.[29] The question is which mechanisms are behind the processes leading to a reduction of electron concentration at the TiO_2 anatase surfaces. Considering the conditions of the experiments, a decrease of the electron concentration can occur when (i) the concentration of oxygen vacancies decreases, (ii) electrons are trapped at localized states, induced by incorporation of carbon species in the TiO_2 lattice, and (iii) absorption of O−H complexes at the sample surface inducing capture of charge carriers from the TiO_2 surface. With respect to mechanism (i), an increased amount of AcacH in the precursor solution leads to more fuel for the combustion process, first, at the stage of the TiO_2 film deposition by USP at 350 °C in air, and second, during crystallization of the layers in the subsequent air treatment at 500 °C. The latest process is more intensive, in which the oxygen partial pressure $P(O_2)$ practically remains constant (considering the open atmospheric conditions), whereas the partial pressures of CO_2 and H_2O can significantly increase by increased temperature of AcacH-assisted combustion process. It is likely that a higher temperature and higher CO_2 partial pressures can raise oxygen chemical potentials that could lead to a reduction of the V_O concentration, thereby causing a decrease of the free electron concentration. (ii) On the other hand, within the same process, the carbon impurity incorporates into the lattice and probably also accumulates at the grain boundaries of TiO_2, as suggested by cumulative results of XRD peak shift and XPS and SIMS analysis (Figures S5, S6, and S2). Incorporation of carbon atoms into the lattice of anatase TiO_2 can occur through a substitutional mechanism at the oxygen sites[30] or by taking an interstitial site.[31,32] Thus, the carbon impurity may introduce localized states[33] through which the electrons are trapped and thereby, decreasing the overall electron concentration. (iii) While the former mechanisms can occur at the surface and in the bulk of the samples, transient SPV measurements are surface sensitive, and a change of the surface composition or surface chemistry could also result in the observed decreased electron concentration. Since the SPV measurements are performed in air, it is conceivable that the adsorption of O−H groups could be responsible for the decrease of the electron concentration. Initially, neutral O−H complexes could adsorb on the sample surface, and subsequently, they could capture charge carriers from the TiO_2 surface region thereby effectively reduce the surface electron concentration. However, to elucidate the exact microscopic mechanism responsible for the reduction of electrons at the sample surface additional measurements are required.

4. CONCLUSIONS

Due to transport limitation across grain boundaries and symmetry of charge selectivity embedded by neighbored grains in anatase TiO_2, fast charge separation was related to charge transfer within the anatase TiO_2 crystallites closest to the external surface (first monolayer). The negative and positive stretched exponentials belonged to relaxation of photogenerated electrons and holes separated in space within the duration time of the laser pulse (fast charge separation). The correlation between the amplitudes of the Urbach tails (positive component at long times) and the photocatalytic activity gave evidence that fast separation of photogenerated holes was caused by hole transfer toward the external surface. Furthermore, the correlation of the decreasing τ_e with an increasing photocatalytic degradation rate under both ultraviolet and visible light gave evidence that electrons separated toward the external surface strongly limited the photocatalytic activity for oxidation of organic molecules with anatase nanoparticles. It was demonstrated that an increased amount of AcacH in the TTIP solution led to a passivation of electron traps at the anatase surface and to a reduction of the electron back transfer rate. Suitable mechanisms of AcacH-induced passivation of electron traps at TiO_2 surfaces were analyzed and discussed, providing new and complementary insights in understanding the electronic processes in photocatalytic systems and related buried interfaces.

https://doi.org/10.1021/acsami.2c09032
ACS Appl. Mater. Interfaces 2022, 14, 43163−43170

ASSOCIATED CONTENT

Supporting Information

The Supporting Information is available free of charge at https://pubs.acs.org/doi/10.1021/acsami.2c09032.

Contact angles of anatase TiO_2 thin films, reversible activation of anatase TiO_2 thin films under illumination with UV light, carbon content in anatase TiO_2 thin films, photon flux spectrum in transient SPV spectroscopy, the structural properties of TiO_2 thin films, and the C 1s core level of TiO_2 thin films (PDF)

AUTHOR INFORMATION

Corresponding Authors

Thomas Dittrich − *Helmholtz Zentrum Berlin für Materialien und Energie GmbH, Institut für Silizium-Photovoltaik, D-12489 Berlin, Germany;* orcid.org/0000-0002-2698-9481; Email: dittrich@helmholtz-berlin.de

Nicolae Spalatu − *Tallinn University of Technology, Department of Materials and Environmental Technology, 19086 Tallinn, Estonia;* orcid.org/0000-0003-0234-2170; Email: nicolae.spalatu@taltech.ee

Authors

Jekaterina Sydorenko − *Tallinn University of Technology, Department of Materials and Environmental Technology, 19086 Tallinn, Estonia;* orcid.org/0000-0001-7675-0471

Norbert H. Nickel − *Helmholtz Zentrum Berlin für Materialien und Energie GmbH, Institut für Silizium-Photovoltaik, D-12489 Berlin, Germany*

Arvo Mere − *Tallinn University of Technology, Department of Materials and Environmental Technology, 19086 Tallinn, Estonia*

Malle Krunks − *Tallinn University of Technology, Department of Materials and Environmental Technology, 19086 Tallinn, Estonia;* orcid.org/0000-0003-4658-4403

Ilona Oja Acik − *Tallinn University of Technology, Department of Materials and Environmental Technology, 19086 Tallinn, Estonia*

Complete contact information is available at: https://pubs.acs.org/10.1021/acsami.2c09032

Author Contributions

The manuscript was written through contributions of all authors. All authors have given approval to the final version of the manuscript.

Funding

This study was funded by the Estonian Research Council project PRG627 and PSG689. The Estonian Centre of Excellence project TK141 (TAR16016EK). The European Union's Horizon2020 program under the ERA Chair project 5GSOLAR, grant agreement No 952509.

Notes

The authors declare no competing financial interest.

ABBREVIATIONS

SPV, surface photovoltage; AcAcH, acetylacetone; TTIP, titanium(IV)isopropoxide; CPD, contact potential difference

REFERENCES

(1) Fujishima, A.; Honda, K. Electrochemical Photolysis of Water at a Semiconductor Electrode. *Nature* **1972**, *238*, 37.

(2) Etacheri, V.; Di Valentin, C.; Schneider, J.; Bahnemann, D.; Pillai, S. C. Visible-Light Activation of TiO_2 Photocatalysts: Advances in Theory and Experiments. *Journal of Photochemistry and Photobiology C: Photochemistry Reviews.* **2015**, *25*, 1.

(3) Navidpour, A. H.; Hosseinzadeh, A.; Zhou, J. L.; Huang, Z. Progress in the Application of Surface Engineering Methods in Immobilizing TiO_2 and ZnO Coatings for Environmental Photocatalysis. *Catal. Rev. - Sci. Eng.* **2021**, 1.

(4) Banerjee, S.; Dionysiou, D. D.; Pillai, S. C. Self-Cleaning Applications of TiO_2 by Photo-Induced Hydrophilicity and Photocatalysis. *Appl. Catal. B: Environmental.* **2015**, *176-177*, 396.

(5) Pan, F.; Wu, K.; Li, H.; Xu, G.; Chen, W. Synthesis of {100} Facet Dominant Anatase TiO_2 Nanobelts and the Origin of Facet-Dependent Photoreactivity. *Chem. - A Eur. J.* **2014**, *20* (46), 15095−15101.

(6) Stefanov, B. I.; Niklasson, G. A.; Granqvist, C. G.; Österlund, L. Gas-Phase Photocatalytic Activity of Sputter-Deposited Anatase TiO_2 Films: Effect of (0 0 1) Preferential Orientation, Surface Temperature and Humidity. *J. Catal.* **2016**, *335*, 187.

(7) Quirk, J. A.; Miao, B.; Feng, B.; Kim, G.; Ohta, H.; Ikuhara, Y.; McKenna, K. P. Unveiling the Electronic Structure of Grain Boundaries in Anatase with Electron Microscopy and First-Principles Modeling. *Nano Lett.* **2021**, *21*, 9217.

(8) Dagdeviren, O. E.; Glass, D.; Sapienza, R.; Cortés, E.; Maier, S. A.; Parkin, I. P.; Grütter, P.; Quesada-Cabrera, R. The Effect of Photoinduced Surface Oxygen Vacancies on the Charge Carrier Dynamics in TiO_2 Films. *Nano Lett.* **2021**, *21*, 8348.

(9) Sano, T.; Puzenat, E.; Guillard, C.; Geantet, C.; Matsuzawa, S.; Negishi, N. Improvement of Photocatalytic Degradation Activity of Visible-Light- Responsive TiO_2 by Aid of Ultraviolet-Light Pretreatment. *J. Phys. Chem. C* **2009**, *113*, 5535.

(10) Chang, C. H.; Chuang, C. H.; Zhong, D. Y.; Lin, J. C.; Sung, C. C.; Hsu, C. Y. Synthesized TiO_2 Mesoporous by Addition of Acetylacetone and Graphene for Dye Sensitized Solar Cells. *Coatings* **2021**, *11*, 796.

(11) Byrne, C.; Fagan, R.; Hinder, S.; McCormack, D. E.; Pillai, S. C. New Approach of Modifying the Anatase to Rutile Transition Temperature in TiO_2 Photocatalysts. *RSC Adv.* **2016**, *6* (97), 95232−95238.

(12) Juma, A. O.; Acik, I. O.; Mikli, V.; Mere, A.; Krunks, M. Effect of Solution Composition on Anatase to Rutile Transformation of Sprayed TiO_2 Thin Films. *Thin Solid Films* **2015**, *594*, 287.

(13) Kaltsum, U.; Kurniawan, A. F.; Nurhasanah, I.; Priyono, P. The Role of Concentration Ratio of TTiP: AcAc on the Photocatalytic Activity of TiO_2 Thin Film in Reducing Degradation Products of Used Frying Oil. *Bull. Chem. React. Eng. & Catal.* **2017**, *12* (3), 430−436.

(14) Siwińska-Stefańska, K.; Zdarta, J.; Paukszta, D.; Jesionowski, T. The Influence of Addition of a Catalyst and Chelating Agent on the Properties of Titanium Dioxide Synthesized via the Sol−Gel Method. *J. Sol-Gel Sci. Technol.* **2015**, *75*, 264−278.

(15) Spiridonova, J.; Katerski, A.; Danilson, M.; Krichevskaya, M.; Krunks, M.; Oja Acik, I. Effect of the Titanium Isopropoxide:Acetylacetone Molar Ratio on the Photocatalytic Activity of TiO_2 Thin Films. *Molecules* **2019**, *24*, 4326.

(16) Kronik, L.; Shapira, Y. Surface Photovoltage Phenomena: Theory, Experiment, and Applications. *Surf. Sci. Rep.* **1999**, *37*, 1.

(17) Dittrich, T.; Valle Rios, L. E.; Kapil, S.; Gurieva, G.; Rujisamphan, N.; Schorr, S. Temperature Dependent Transient Surface Photovoltage Spectroscopy of a $Cu_{1.95}Zn_{1.1}Sn_{0.96}Se_4$ Kesterite Single Phase Powder. *Appl. Phys. Lett.* **2017**, *110*, 023901.

(18) Fengler, S.; Kriegel, H.; Schieda, M.; Gutzmann, H.; Klassen, T.; Wollgarten, M.; Dittrich, T. Charge Transfer in C-Si(N^{+2})/TiO_2(ALD) at the Amorphous/Anatase Transition: A Transient Surface Photovoltage Spectroscopy Study. *ACS Appl. Mater. Interfaces* **2020**, *12*, 3140.

(19) Dittrich, T.; Fengler, S. *Surface Photovoltage Analysis of Photoactive Materials* **2020**, DOI: 10.1142/q0227.
(20) Dittrich, T.; Fengler, S.; Nickel, N. Surface Photovoltage Spectroscopy over Wide Time Domains for Semiconductors with Ultrawide Bandgap: Example of Gallium Oxide. *Phys. Status Solidi Appl. Mater. Sci.* **2021**, *218*, 2100167.
(21) Hansen, W. N.; Hansen, G. J. Standard Reference Surfaces for Work Function Measurements in Air. *Surf. Sci.* **2001**, *481*, 172.
(22) Spiridonova, J.; Mere, A.; Krunks, M.; Rosenberg, M.; Kahru, A.; Danilson, M.; Krichevskaya, M.; Oja Acik, I. Enhanced Visible and Ultraviolet Light-Induced Gas-Phase Photocatalytic Activity of TiO_2 Thin Films Modified by Increased Amount of Acetylacetone in Precursor Solution for Spray Pyrolysis. *Catalysts* **2020**, *10*, 1011.
(23) Tang, H.; Lévy, F.; Berger, H.; Schmid, P. E. Urbach Tail of Anatase TiO_2. *Phys. Rev. B* **1995**, *52*, 7771.
(24) Baldini, E.; Chiodo, L.; Dominguez, A.; Palummo, M.; Moser, S.; Yazdi-Rizi, M.; Auböck, G.; Mallett, B. P. P.; Berger, H.; Magrez, A.; Bernhard, C.; Grioni, M.; Rubio, A.; Chergui, M. Strongly Bound Excitons in Anatase TiO_2 Single Crystals and Nanoparticles. *Nat. Commun.* **2017**, DOI: 10.1038/s41467-017-00016-6.
(25) Jellison, G. E.; Boatner, L. A.; Budai, J. D.; Jeong, B. S.; Norton, D. P. Spectroscopic Ellipsometry of Thin Film and Bulk Anatase (TiO_2). *J. Appl. Phys.* **2003**, *93*, 9537.
(26) Fengler, S.; Zillner, E.; Dittrich, T. Density of Surface States at CdSe Quantum Dots by Fitting of Temperature-Dependent Surface Photovoltage Transients with Random Walk Simulations. *J. Phys. Chem. C* **2013**, *117*, 6462.
(27) Kytin, V.; Duzhko, V.; Timoshenko, V. Y.; Rappich, J.; Dittrich, T. Injection Photovoltage in Thin Anodic TiO_2 Layers. *Phys. Status Solidi Appl. Res.* **2001**, *185*, R1.
(28) Timoshenko, V. Y.; Duzhko, V.; Dittrich, T. Diffusion Photovoltage in Porous Semiconductors and Dielectrics. *Phys. Status Solidi Appl. Res.* **2000**, *182*, 227.
(29) Deák, P.; Aradi, B.; Frauenheim, T. Quantitative Theory of the Oxygen Vacancy and Carrier Self-Trapping in Bulk TiO_2. *Phys. Rev. B* **2012**, DOI: 10.1103/PhysRevB.86.195206.
(30) Lee, J. C.; Gopalan, A. I.; Saianand, G.; Lee, K. P.; Kim, W. J. Manganese and Graphene Included Titanium Dioxide Composite Nanowires: Fabrication, Characterization and Enhanced Photocatalytic Activities. *Nanomaterials* **2020**, *10*, 456.
(31) Matysina, Z. A.; Zaginaichenko, S. Y.; Schur, D. V. Hydrogen Solubility in Alloys under Pressure. *Int. J. Hydrogen Energy* **1996**, *21*, 1085.
(32) Zhao, H.; Pan, F.; Li, Y. A Review on the Effects of TiO_2 Surface Point Defects on CO_2 Photoreduction with H_2O. *Journal of Materiomics.* **2017**, *3*, 17.
(33) Di Valentin, C.; Pacchioni, G.; Selloni, A. Theory of Carbon Doping of Titanium Dioxide. *Chem. Mater.* **2005**, *17*, 6656.